

Switching Time Analysis of Negative Capacitance UTB GeOI MOSFETs

Pin-Chieh Chiu and Vita Pi-Ho Hu

Department of Electrical Engineering, National Central University, Taoyuan, Taiwan

Phone: +886-3-4227151 Email: vitahu@ee.ncu.edu.tw

Abstract

In this work, the impact of device parameters on the switching time and subthreshold swing of negative capacitance ultra-thin-body (UTB) Germanium-On-Insulator (NC-GeOI) MOSFETs is analyzed. NC-GeOI MOSFETs with smaller gate length (L_g), EOT, and buried oxide thickness (T_{box}) and thicker ferroelectric layer thickness (T_{FE}) exhibit larger subthreshold swing improvements over GeOI MOSFETs. Compared with GeOI MOSFETs, NC-GeOI MOSFETs exhibit better switching time due to improvements in effective drive current (I_{eff}) and subthreshold swing. NC-GeOI MOSFET exhibits larger ST improvements at $V_{\text{dd}} = 0.3\text{V}$ (-82.9%) than at $V_{\text{dd}} = 0.86\text{V}$ (-9.7%), because NC-GeOI MOSFET shows 18.2 times higher I_{eff} than the GeOI MOSFET at $V_{\text{dd}} = 0.3\text{V}$, while 2.5 times higher I_{eff} at $V_{\text{dd}} = 0.86\text{V}$. Therefore, NC-GeOI MOSFETs have more benefits when operating at low supply voltage for ultra-low power applications.

Introduction

The design of ultra-low power integrated circuits is important for portable electronics, implantable bio-medical devices, and energy harvesting system. Device with higher $I_{\text{on}}/I_{\text{off}}$ ratio is essential in order to achieve energy-efficient switching at given supply voltage. Negative capacitance FET (NCFET) [1] has been attracting interests because it reduces subthreshold swing below classical limit of $\sim 60\text{mV/dec}$, and therefore shows higher $I_{\text{on}}/I_{\text{off}}$ ratio. Negative capacitance ultra-thin-body MOSFETs (NC-UTB MOSFETs) have been analyzed for capacitance tuning and antiferroelectric operation [2-3]. The hysteresis-free design space for NC-UTB GeOI MOSFETs has been studied compared with Si counterparts [4]. However, switching time (ST) analysis of NC-GeOI MOSFET has rarely been discussed. In this work, the impact of device parameters (including L_g , EOT and T_{box}) and thickness of ferroelectric layer (T_{FE}) on the subthreshold swing (SS) and ST of the hysteresis-free NC-GeOI MOSFETs are analyzed and compared with the GeOI MOSFETs. Mobility and band-to-band tunneling model of UTB GeOI MOSFET are calibrated [6] in the TCAD simulations. Results show that compared with the GeOI MOSFETs at $V_{\text{dd}} = 0.86\text{V}$, the NC-GeOI MOSFETs exhibit significant improvements in SS while fewer improvements in ST due to the increased transition charge (ΔQ). However, as V_{dd} scales down to 0.3V , NC-GeOI MOSFETs show larger improvements in ST due to much higher I_{eff} improvements.

Subthreshold Swing of NC-GeOI MOSFETs

Fig. 1(a) illustrates the 2D NC-GeOI structure used in this work. Fig. 1(b) shows the I_d - V_g characteristics of the baseline GeOI and NC-GeOI MOSFETs. The ferroelectric parameters of $\text{Hf}_{0.5}\text{Zr}_{0.5}\text{O}_2$ ferroelectric layer, such as coercive electric field $E_c = 1\text{ MV/cm}$, remnant polarization $P_0 = 17\text{ }\mu\text{C/cm}^2$ [8] and $T_{\text{FE}} = 8\text{ nm}$, are used for NC-GeOI MOSFETs with hysteresis-free design. Fig. 2 shows the simulation flow of 2D TCAD coupled with 1D Landau-Khalatnikov (LK) ferroelectric equation for modeling the NC-GeOI MOSFETs [5]. Fig. 3 describes the simple capacitance model of NC-GeOI MOSFET and equations for analyzing the internal voltage amplification (A_v), subthreshold swing (SS) and switching time (ST). According to the definition of internal voltage amplification (A_v), capacitance underneath the ferroelectric layer (C_{mos}) should be closer to the capacitance of ferroelectric layer $|C_{\text{FE}}|$ in order to achieve higher A_v and smaller SS of NC-GeOI MOSFETs. However, $|C_{\text{FE}}|$ cannot be smaller than C_{mos} to avoid hysteresis phenomenon. At external gate voltage of NC-GeOI MOSFET ($V_{g,\text{ext}} = 0\text{ V}$), $|C_{\text{FE}}|$ can be described as $C_{\text{FE}} = dQ_g/dV_{\text{FE}} \approx 1/(2\alpha \cdot T_{\text{FE}})$.

The gate charge (Q_g) at $V_{g,\text{ext}} = 0\text{ V}$ is too small that the second term of V_{FE} shown in Fig. 2 can be ignored. The simplified equation of C_{FE} indicates that $|C_{\text{FE}}|$ is only related to ferroelectric parameters at low $V_{g,\text{ext}}$. Therefore, the C_{mos} is the key of capacitance matching for achieving better SS. Fig. 4 shows the impact of device parameters on

the C_{mos} , $|C_{\text{FE}}|$ and SS for GeOI and NC-GeOI MOSFETs at $V_{\text{ds}} = 0.05\text{ V}$. The inset of Fig. 4(a) shows that C_{mos} increases as L_g decreases from 100 nm to 20.2 nm . Therefore, the SS improvements of NC-GeOI MOSFETs over GeOI MOSFETs increase as L_g decreases. Compared with the GeOI MOSFETs, NC-GeOI MOSFETs show 32.7% (9%) SS improvements at $L_g = 20.2\text{ nm}$ ($L_g = 100\text{ nm}$). The SS improvement is defined as $[(SS_{\text{NC-GeOI}} - SS_{\text{GeOI}})/SS_{\text{GeOI}}]$. The inset of Fig. 4(b) shows that $|C_{\text{FE}}|$ decreases as T_{FE} increases. Therefore, the SS improvements increase with T_{FE} . With $T_{\text{FE}} = 8\text{ nm}$, the NC-GeOI MOSFET shows 32.3% SS improvement. The inset of Fig. 4(c) shows that for NC-GeOI MOSFETs, reducing EOT increases C_{mos} , and therefore exhibits slightly larger SS improvement as EOT decreases. Decreasing T_{box} shows slightly larger C_{mos} and SS improvement as shown in Fig. 4(d).

Switching Time of NC-GeOI MOSFETs

In this section, the impact of device parameters on the switching time (ST) of NC-GeOI MOSFETs compared with GeOI MOSFETs is analyzed. The switching time is defined as $ST = \Delta Q / I_{\text{eff}}$ [7], where ΔQ is the transition charge between "on" and "off" states and given by the difference between Q_g ($V_g = V_{\text{dd}}$, $V_d = 0.05V$) and Q_g ($V_g = 0$, $V_d = V_{\text{dd}}$). I_{eff} is the effective drive current which is given by the average of I_d ($V_g = V_{\text{dd}}$, $V_d = V_{\text{dd}}/2$) and I_d ($V_g = V_{\text{dd}}/2$, $V_d = V_{\text{dd}}$). Fig. 5 (a) shows the impact of T_{FE} on the ST of NC-GeOI MOSFETs compared with GeOI MOSFETs. It can be seen that compared with GeOI MOSFET, NC-GeOI MOSFETs with thicker T_{FE} exhibit smaller ST and larger improvements in ST (17.7% at $T_{\text{FE}} = 10\text{ nm}$). This is because as T_{FE} increases, the increase in I_{eff} is more significant than the increase in ΔQ for NC-GeOI MOSFETs as shown in Fig. 5(b). Reducing EOT improves the SS of NC-GeOI MOSFETs (Fig. 4(c)). However, Fig. 6(a) shows that reducing EOT slightly increases the ST of NC-GeOI MOSFETs. This is because as EOT decreases, the increase in ΔQ is slightly higher than the increase in I_{eff} for NC-GeOI MOSFETs as shown in Fig. 6(b). Besides, the ST of GeOI MOSFETs slightly increases with EOT because the reductions of I_{eff} is slightly larger than the reduction in ΔQ as EOT increases. In other words, NC-GeOI MOSFETs exhibit better ST as EOT increases, although SS decreases with EOT. Fig. 7(a) shows that the ST of GeOI and NC-GeOI MOSFETs increase as T_{box} decreases because the I_{eff} degrades intensely with reducing T_{box} (Fig. 7(b)). Compared to GeOI MOSFET with $T_{\text{box}} = 2\text{ nm}$, NC-GeOI MOSFET still shows smaller ST (59.3% improvement in ST) because of larger I_{eff} . Fig. 8(a) and 8(b) show the impact of L_g on the ST of GeOI and NC-GeOI MOSFETs at $V_{\text{dd}} = 0.86\text{V}$ and $V_{\text{dd}} = 0.3\text{V}$, respectively. As L_g decreases, ST decreases due to decreasing ΔQ and increasing I_{eff} . Compared with GeOI MOSFETs at $V_{\text{dd}} = 0.86\text{V}$, NC-GeOI MOSFETs show 36.1% improvement in ST at $L_g = 100\text{ nm}$ and 9.7% improvement in ST at $L_g = 20.2\text{ nm}$. Compared with GeOI MOSFET with $L_g = 20.2\text{ nm}$, NC-GeOI MOSFET exhibits significant ST improvement at $V_{\text{dd}} = 0.3\text{V}$ (-82.9%) and slightly ST improvement at $V_{\text{dd}} = 0.86\text{V}$ (-9.7%). This is because at $V_{\text{dd}} = 0.3\text{V}$ and $L_g = 20.2\text{ nm}$, NC-GeOI MOSFET exhibits 18.2 times higher I_{eff} than the GeOI MOSFET; while at $V_{\text{dd}} = 0.86\text{V}$, NC-GeOI MOSFET shows 2.5 times larger I_{eff} than the GeOI MOSFET. In other words, NC-GeOI MOSFETs show more benefits when operating at low supply voltage.

Acknowledgments

This work is supported by the Ministry of Science and Technology in Taiwan under Contracts MOST 105-2628-E-008-006-MY3 and 105-2622-8-002-001.

References

- [1] S. Salahuddin et al., *Nano Lett.*, vol. 8, pp. 405, 2008.
- [2] Asif I. Khan et al., *IEDM*, p. 11.3.1, 2011.
- [3] Chun Wing Yeung et al., *VLSI-TSA*, 2013.
- [4] Ho-Pei Lee et al., *VLSI-TSA*, 2017.
- [5] Pin-Chieh Chiu et al., *IEEE EDTM*, 2017.
- [6] Tony Low et al., *Appl. Phys. Lett.*, 85, 2402, 2004.
- [7] Steven E. Laux et al., *IEEE TED*, p. 2304-2320, 2007.
- [8] Johannes Muller et al., *Nano Lett.*, 12 (8), 4318-4323, 2012.

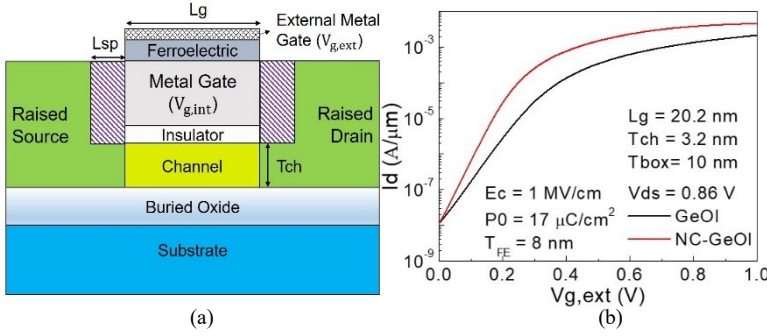


Fig. 1. (a) The 2D NC-GeOI structure used in this work. $V_{g,ext}$ is the voltage of external metal gate. $V_{g,int}$ is the voltage of internal metal gate. (b) The I_d - V_g characteristics of the TCAD baseline UTB-GeOI and NC-GeOI MOSFETs. The NC-GeOI is modeled based on the baseline GeOI and LK equation. At $V_{ds} = 0.86$ V, NC-GeOI and GeOI MOSFETs are designed to have the same I_{off} for a fair comparison. The ferroelectric parameters are extracted from $Hf_{0.5}Zr_{0.5}O_2$. [8]

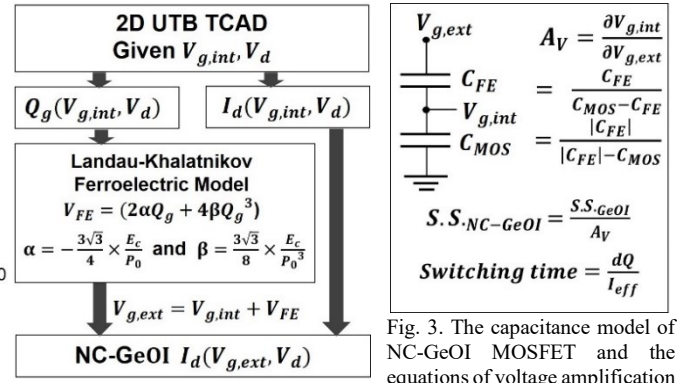


Fig. 2. 2D TCAD GeOI MOSFET simulation coupled with 1D-LK equation is used to model NC-GeOI MOSFET. [5]

$$V_{g,ext} = V_{g,int} + V_{FE}$$

$$A_V = \frac{\partial V_{g,int}}{\partial V_{g,ext}} = \frac{C_{FE}}{C_{MOS} - C_{FE}} = \frac{C_{FE}}{|C_{FE}| - C_{MOS}}$$

$$S.S._{NC-GeOI} = \frac{S.S._{GeOI}}{A_V}$$

$$\text{Switching time} = \frac{dQ}{I_{eff}}$$

Fig. 3. The capacitance model of NC-GeOI MOSFET and the equations of voltage amplification factor (A_V), subthreshold swing (S.S.), and switching time. I_{eff} is the effective current and dQ is the transition charge [7].

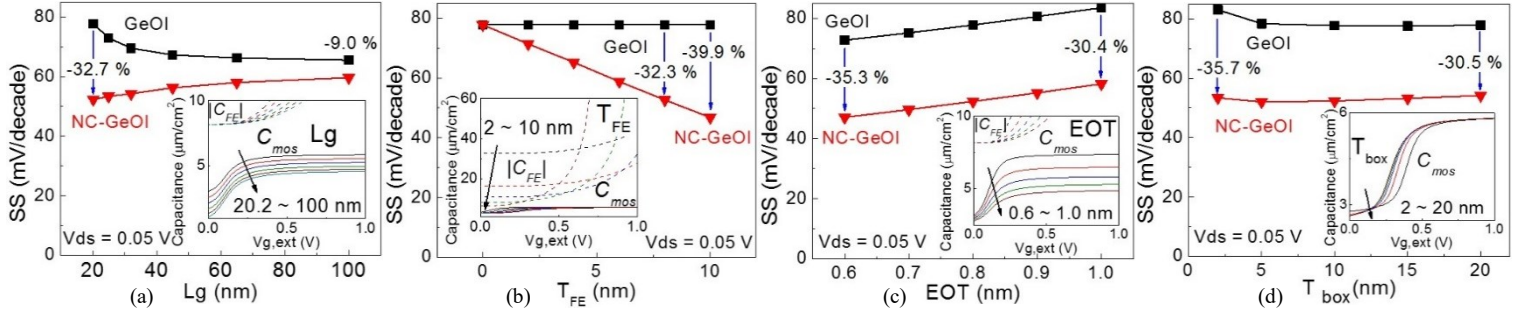


Fig. 4. Impacts of (a) L_g , (b) T_{FE} , (c) EOT and (d) T_{box} on the SS and the capacitances at $V_{ds} = 0.05$ V. C_{mos} is the capacitance of the device underneath the ferroelectric layer and $|C_{FEI}|$ is the capacitance of ferroelectric layer. For NC-GeOI MOSFET at $V_{g,ext} = 0$ V, C_{mos} should be close to its $|C_{FEI}|$ to achieve higher A_V and larger improvement in SS compared to the baseline GeOI MOSFET.

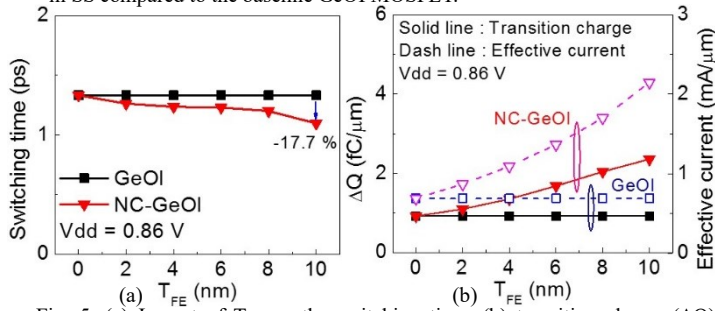


Fig. 5. (a) Impact of T_{FE} on the switching time, (b) transition charge (ΔQ) and effective current (I_{eff}). NC-GeOI MOSFETs with thicker T_{FE} show lower switching time than GeOI MOSFETs, because NC-GeOI MOSFETs show much larger I_{eff} in spite of larger ΔQ compared with the GeOI MOSFETs.

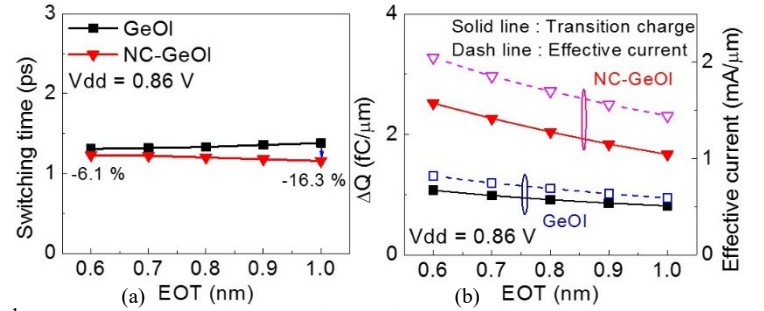


Fig. 6. (a) Impact of EOT on the switching time, (b) ΔQ and I_{eff} . As EOT scales, NC-GeOI MOSFETs show slightly increase in switching time because the increase in ΔQ is more than the increase in I_{eff} as EOT reduces.

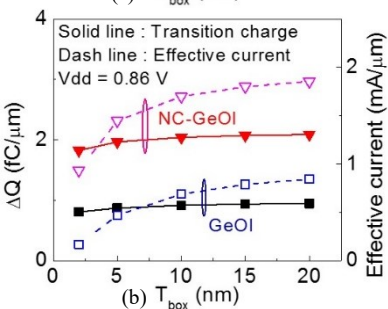
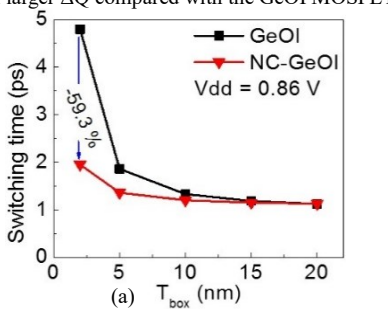


Fig. 7. (a) Impact of T_{box} on the switching time, (b) ΔQ and I_{eff} . GeOI and NC-GeOI MOSFETs with thinner T_{box} show larger switching time because of degraded I_{eff} . Compared to GeOI MOSFET with $T_{box} = 2$ nm, NC-GeOI MOSFET still exhibits better switching time due to larger I_{eff} .

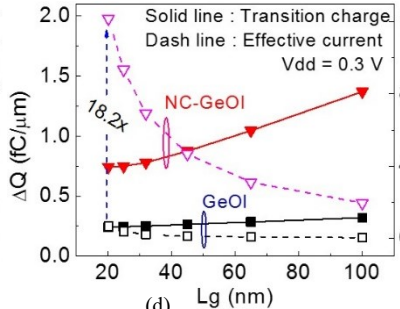
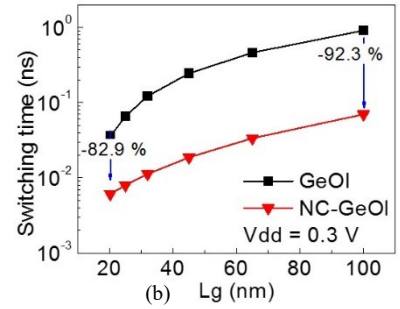
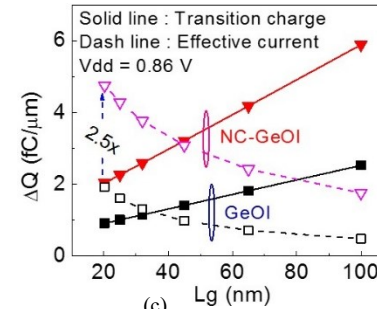
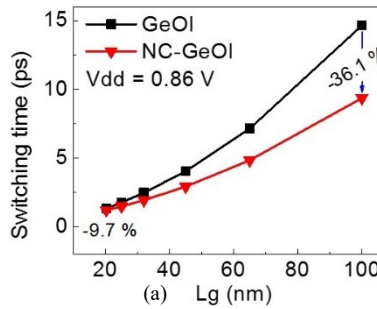


Fig. 8. Impact of L_g on the switching time at (a) $V_{dd} = 0.86$ V and (b) at $V_{dd} = 0.3$ V. Impact of L_g on the ΔQ and I_{eff} at (c) $V_{dd} = 0.86$ V and (d) at $V_{dd} = 0.3$ V. With $L_g = 20.2$ nm and compared with GeOI MOSFET, NC-GeOI MOSFET shows 9.7% improvement in switching time at $V_{dd} = 0.86$ V, and 82.9% improvement in switching time at $V_{dd} = 0.3$ V. NC-GeOI MOSFET exhibits significant advantages in switching time at low V_{dd} compared with the GeOI MOSFET.